THE ASTROPHYSICAL JOURNAL, 249:241–253, 1981 October 1

INTERPULSE EMISSION FROM PULSAR 0950+08: HOW MANY POLES?

T. H. HANKINS
Arecibo Observatory
AND
J. M. CORDES
Cornell University
Received 1980 December 15; accepted 1981 April 8

ABSTRACT

We discuss the frequency dependence of emission over the entire pulse period and find that: (1) interpulse emission is accompanied by low level emission over at least 83% of the rotation period; (2) individual interpulses are occasionally as strong as 60% of the average main pulse compared to an average interpulse–main pulse ratio of 2%; (3) interpulses are correlated with main pulses; (4) the interpulse–main pulse separation is frequency independent between 100 and 5000 MHz; whereas (5) the average interpulse and main pulse widths vary as $\nu^{-0.5\pm0.05}$ below 400 MHz.

We discuss whether main pulses and interpulses arise from opposite magnetic poles or form a single magnetic pole. Both models are found to have difficulties, but double-pole models appear less realistic than single-pole models. A double-pole model requires a unidirectional communication between poles and is in conflict with polarization measurements. In a single-pole model, it is implausible—within the context of known pulsar phenomenology—that the interpulse and main pulse correspond to the intense portions of a hollow cone beam because of item (4) above. We discuss modifications of single-pole models that would resolve their present incompatibility with observation.

Subject headings: pulsars — radiation mechanisms

I. INTRODUCTION

We discuss in detail the emission from PSR 0950+08, the first pulsar in which an interpulse was discovered (Rickett and Lyne 1968). The interpulse, whose separation from the main pulse is $\sim 152°$ of longitude (360° = one pulse period), was first interpreted as emission from a magnetic pole opposite to that responsible for the main pulse. Later, Manchester and Lyne (1977) proposed that all emission may arise from a single magnetic pole, a notion that subsequently has received theoretical support (e.g., Arons 1979). At present, pulsars as a class display emission components with an apparent continuum of separations (Manchester 1978), which suggests that interpulse–main pulse emission is totally analogous to double-lobed average pulse shapes with much smaller lobe separations.

In this paper we discuss the relationship of the main pulse and interpulse by considering the frequency dependence of the average pulse profile over 2 decades of frequency (100 to 5000 MHz) and by investigating the average polarization behavior and pulse-to-pulse fluctuations. The data do not unequivocally support either the single-pole or double-pole models.

Section II describes the observations of single pulses that we made at 430 MHz and form the heart of our study of pulse fluctuations in § IV. Section III discusses the frequency dependence of the interpulse and main pulse, the existence of emission over at least 83% of the rotation period, and summarizes polarization measurements. Section IV establishes that interpulse and main pulse amplitudes are correlated. Section V discusses single-pole and double-pole models from a phenomenological standpoint. We end the paper with a more general discussion in § VI and a summary of our conclusions.

II. OBSERVATIONS

Unpublished single-pulse data discussed below were obtained with the 305 m telescope at the Arecibo Observatory. Measurements at 430 MHz with sampling through the entire pulse period were obtained in 1976 April and are discussed in detail in § IV. Both circular polarizations were sampled at 1 ms intervals in 2 MHz bandwidths and with 3.3 ms time constants. The system temperature was 150°, thus yielding an uncertainty ~ 0.1 Jy per independent sample. Measurements from 120 to 400 MHz were obtained in 1978 December and 1979 November using a frequency-agile receiver that allowed single-pulse measurements at four frequencies simultaneously (Cordes and Rickett 1981). Average profiles of the total intensity reported from this program in § III were calculated from data with a 0.5 MHz bandwidth and 1.0 ms time constant.

The remaining data discussed in § III were taken from the literature or were graciously provided by various colleagues and are listed in Table 1.

III. AVERAGE PROFILES

a) Frequency Dependence

We have assembled a number of average profiles over the frequency range of 40 to 8000 MHz. Table 1 lists the

TABLE 1

COMPONENT WIDTHS AND SEPARATIONS

Frequency	Date	Time Res. (ms)	No. of Pulses	Interpulse To Main Pulse Sep (°)	Interpulse FWHM(°)	Main Pulse FWHM(°)	Main Pulse Component Separation(°)	Ref.
40.12	21 Feb 69	1	19520	153°±17	21°.7	39.8	26°.1	1
46.8	5 May 80	4.8	11850	156 ±18	21.3±5.2	34.2±4	17±5	2
61.2		5				29±12	14.3±2	3
102.5		2	∿7500			23±8.8		3
73.8	14 May 69	5	17486	156.5±5				1
111.5	24 Aug 68	1	3012	156.0±1			10.8	1
111.5	03 Jul 69	0.5				18.4	9.5	1
111.5	1 Dec 70	0.056	700			17.2	9.7	4
111.5	28 Mar 72	0.028	700			18.0	9.8	5
111.5	16 Feb 76	0.66	3600				8.5	2
111.5	18 Feb 76	0.056	700			19.0	10.4	2
125.79	15 Dec 78	0.5	600			17.4±2	10.2±2	6
130.04	15 Dec 78	0.5	600			16.6±1.1	8.8±1.2	6
134.74	15 Dec 78	0.5	600			18.0±1.3	8.3±0.9	6
140.00	15 Dec 78	0.5	600			17.8±1.2	7.1±1.2	6
151.0		4.0				20.0±1	6.5±1	7
207.23	07 Dec 78	1.4	600			16.5±2		6
214.95	22 Nov 79	1.2	600			16.2±2	5.8±1.6	6
228.05	07 Dec 78	1.4	600			15.1±2		6
238.47	22 Nov 79	1.2	600			16.5±2	6.3±0.8	6
240.0		4.0				14.2±2	5.3±1	7
256.75	07 Dec 79	1.0	600			14.5±2		7
262.0	14 Nov 77	0.056	600			14.4±1	5.1±1	2
271.9	22 Nov 79	1.0	600			15.6±1	6.1±0.9	7
300.0	07 Dec 79	1.0	600			14.0±1		7
318	28 Mar 72	0.028	700			13.0±1	6.5±1	5
325.0	22 Nov 79	1.0	600			14.4±1	5.0+1	7
400	1971-72	0.25				14.0±1		8
408					23.6±2	12.0±1		7
430	21 Feb 69	1.0	9760	147.5±2	27.5±2	13.3±1		1
430	1971-74	1.0	27578		25.6±0.6	13.2±0.4		9
430			13600	153.8±2	28±2			10
430	28 Jan 73	0.5	822	149.6±1	27.2	13.6±1		11
430	26 Apr 76	3.3	16000	146.4±1				12
430	15 May 76	0.016	400			11.8±1		13
430	Feb 1980	0.1	10177			12.9±1.0		14
430	14 May 80	0.55	16597			12.9±1.3		2
430	24 May 80	0.55	13370	148.3±1		13.8±1		2
610		4.0				13.1±1		7
1380	6 Jul 80	0.2	4050	155.2±1.8	22.5±1	13.5±1		15
1385	13 May 80	0.55	11850	154.5±1.4	20.9±2.0	13.5±0.8		2
1406	Feb 1980	0.04	9148			11.6±0.7		9
1409	7 Apr 76	0.13	2000			11.4±0.3		2
1420	25 Nov 75	5.0	7168	155.2±2		11.9±0.3		16
1665						12.4±0.5		17
1720		1.0	2048		21±1	12.0±0.5		18
2380	15 May 80	0.55	9480	155.8±1.3	20.9±2.0	13.5±0.8		2
2388	1968-1978	1.3	1850000			11.9±1.0		19
2650		1.0	14800	158±2		12.6±1.0		18
2695	05 Jul 75	1.0	11500	157.6±2	18.4±4	12.9±0.5		20
4850	03 Nov 76	1.0	7168	151.2±2	16.8±5	11.0±1		20
4900			>10000	155±2		11.7±1		21
8700		1.0	16384			11.8±1		19

REFERENCES.—(1) Craft 1970; (2) T. H. Hankins, unpublished Arecibo data 1980; (3) Izvekova *et al.* 1979; (4) Hankins 1971; (5) Rickett, Hankins, and Cordes (1975); (6) J. M. Cordes and B. J. Rickett, unpublished Arecibo data 1978, 1979; Lyne, Smith, and Graham 1971; (8) Taylor, Manchester, and Huguenin 1975; (9) J. M. Rankin, D. C. Backer, and D. B. Campbell, Arecibo polarization survey, average of 8 days' data, unpublished 1980; (10) Backer, Boriakoff, and Manchester 1973; (11) V. Boriakoff, unpublished Arecibo data 1973; (12) J. M. Cordes and T. H. Hankins, unpublished Arecibo data 1976; (13) Hankins and Boriakoff 1978; (14) D. C. Ferguson and V. Boriakoff, unpublished Arecibo data 1980; (15) D. Stinebring and J. M. Cordes, unpublished Arecibo data 1980; (16) J. Seiradakis, unpublished Effelsberg data 1979; (17) Manchester 1971; (18) D. Morris, unpublished Effelsberg data 1979; (19) Downs 1979; (20) D. Graham, J. Seiradakis, and W. Sieber, unpublished Effelsberg data 1979; (21) Sieber, Reinecke, and Wielebinski 1975.

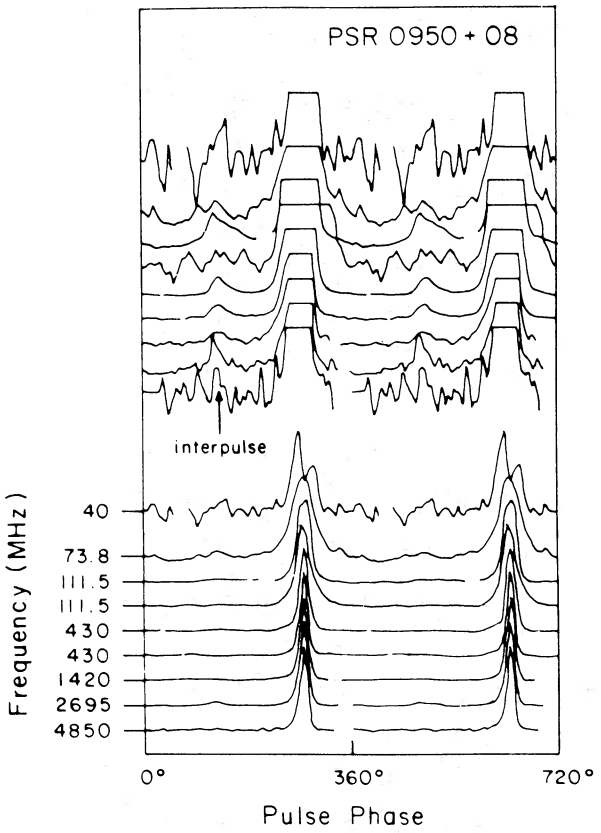

FIG. 1.—Average profiles of PSR 0950+08 at seven frequencies over two full rotation periods. The upper set of profiles has been expanded so as to reveal the interpulse. Gaps in the profiles resulted from the locations of thermal noise pulses or incomplete sampling of the period.

sources of such measurements, and some representative profiles are displayed in Figure 1, where the main pulse and interpulse are evident. The gap in the 111.5 MHz profile results from not having sampled the full period. The zero intensity levels were arbitrarily taken as the mean levels of lowest intensity in 40° and 60° longitude ranges of the pulse period. We discuss below evidence for emission occurring throughout the pulse period. Of immediate interest are the widths and separations of various pulse features and their frequency dependence. The zero levels are unknown, but the asymptotic behavior of the waveforms suggests that nominal zero levels deviate from actual zero levels by no more than 0.1% of the waveform maximum. Consequently, errors in widths and pulse features are dominated by statistical errors such as those discussed below.

In Figure 2 we plot the following quantities versus radio frequency: (1) the half-power main pulse width; (2) the separation of the two components of the main pulse (which appears bifurcated at frequencies below 400 MHz); (3) the half-power interpulse width; and (4) the main pulse–interpulse separation as defined by the interval between midpoints of the half-power levels. Error bars for these curves reflect low signal-to-noise ratios for the interpulse; uncertainties in pulse widths caused by time smearing due to dispersion distortion across the receiver bandwidth or by the postdetection-time constant; and rms deviations of measured widths from a series of measurements with the same receiver system.

Figure 2 indicates that the interpulse and main pulse widths vary as $\nu^{-0.5}$ and $\nu^{-0.47}$, respectively, below 400 MHz. Above that frequency, the main pulse width is practically constant. The separation of the main pulse components varies as $\nu^{-0.68}$ below 400 MHz, above which the components are essentially merged together. In the higher ($\gtrsim$ 400 MHz) frequency range, the bifurcation of the main pulse is evident in profiles of the linearly polarized power, $L \equiv (Q^2 + U^2)^{1/2}$ where Q and U are the Stokes parameters that measure linear polarization (see Cordes and Hankins 1977). We note that the main pulse bifurcation is analogous to the double-lobe behavior or mirror symmetry in pulse fluctuations that is common to many pulsars (Backer 1976). The axis of symmetry is understood to be the magnetic pole in polar cap emission models (Radhakrishnan and Cooke 1969; Komesaroff 1970; Sturrock 1971; Ruderman and Sutherland 1975), and the bifurcation suggests that the radio emission beam is a hollow cone centered on the magnetic axis. The merging of the two components implies that the shape of the hollow cone is frequency dependent. There is considerable evidence (see Cordes 1978) that high (low) frequencies are mapped into small (large) altitudes above the polar cap, and therefore the observed frequency dependence directly reflects the spatial structure of the magnetic polar region. The observed frequency dependencies of the overall main pulse width and interpulse width then suggest that each arises from its own axis of symmetry. That is, on an empirical level where main pulse bifurcations on small ($\lesssim 20°$) longitude scales are common and are commonly associated with a hollow cone beam, it appears that the interpulse and main pulse must arise from different magnetic poles. This conclusion is substantiated by the absence of any frequency dependence of the main pulse–interpulse separation, as is clear in Figure 2 where a line of zero slope is consistent with the data. *We note that the absence of any frequency dependence in a width or separation is extremely unusual*, especially at frequencies below 400 MHz (see width versus frequency curves plotted by Backer 1976). The lack of frequency dependence in the main pulse–interpulse separation suggests that two magnetic poles are required to produce the emission from PSR 0950+08. We discuss this result further (§ V), bringing in additional evidence that apparently contradicts this conclusion.

b) Low Level Emission

Figure 3 shows an average profile of 10^4 pulses at 430 MHz. These data, which were used in the single pulse analysis of the next section, were of exceptional quality, the signal-to-noise ratio of the maximum to rms noise being $\sim 3 \times 10^4$. Low level emission can therefore be examined in these data. The expanded profile in Figure 3 clearly shows the interpulse and the bridge to the main pulse; moreover, emission is evident through *at least* 300°

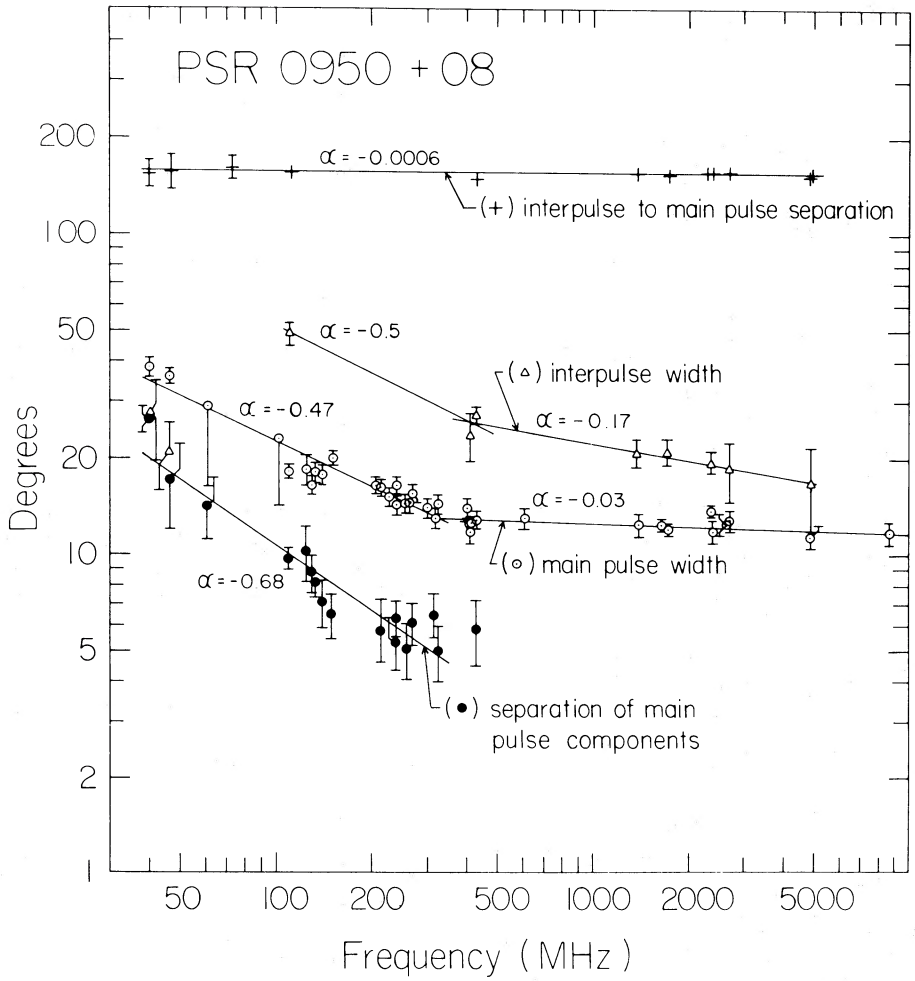

FIG. 2.—Plots of component widths and separations versus frequency. The lines represent unweighted least squares fits to those data points within the line intervals. The power law slopes of the lines are denoted by values of α. The points are listed in Table 1.

of pulse longitude. We are unable to comment on emission through the remaining 60° because a thermal noise calibration signal was fired for 20 ms at the beginning of the sampling window. The minimum intensity levels occur ~30 ms after the end (defined as the e^{-9} point) of the calibration pulse and ~ 77 ms after the peak of the main pulse. It may be fortuitous that these two minimum levels are identical; the true minimum is unknown, and it may be impossible to determine whether emission occurs through the pulse period with a single dish telescope.

c) *Polarization*

Polarization measurements have been a source of primary support for the hollow cone beam model. If the polarization angle is determined by an approximately dipolar magnetic field which, through stellar rotation, changes its orientation, then one would expect a correlation of position angle variation with type of average pulse shape observed. An **S**-shaped variation totaling nearly 180° is expected when the observer's line of sight passes close to the magnetic pole, i.e., when a double pulse shape is observed. In the other extreme, if the line of sight grazes the beam, a single-lobed pulse shape will be seen accompanied by a linear or slightly curved position angle variation over considerably less than 180°. Such a correlation is indeed observed in polarization surveys (Lyne, Smith, and Graham 1971; Manchester 1971; Backer and Rankin 1980).

In Figure 4 we have combined the results of Lyne, Smith, and Graham (1971), Backer and Rankin (1980), and unpublished data to show the position angle variation from the interpulse to the main pulse for PSR 0950+08. The position angle rotates through ~90° in the main pulse, consistent with the merged double-lobe profile at 430 MHz. The position angle rotates continuously through the bridge to the interpulse, with the total rotation being nearly 180°. These data support a single-pole model, as will be discussed in § V.

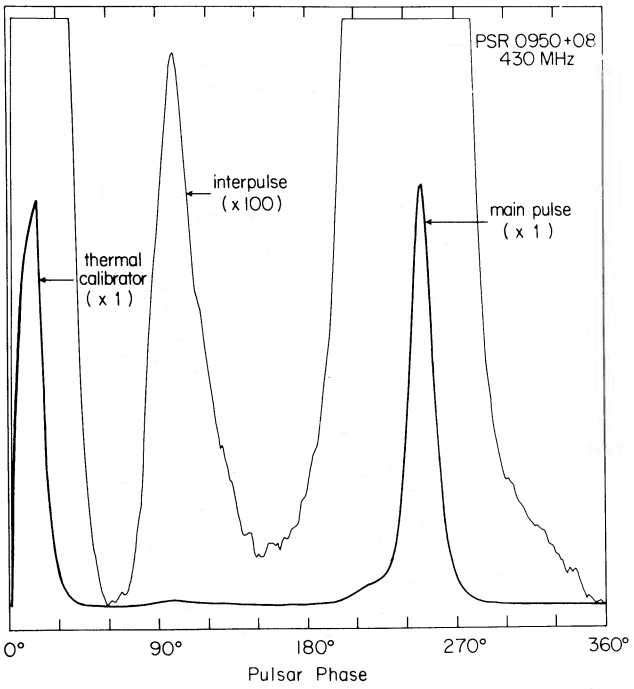

FIG. 3.—Average profile of the total intensity of 430 MHz calculated from 9600 pulses. The expanded (× 100) plot shows emission over at least 300° of longitude.

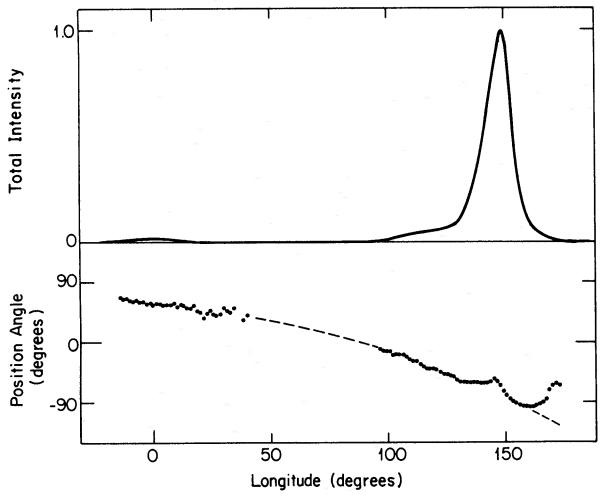

FIG. 4.—Average profile of the total intensity and the polarization position angle of PSR 0950+08 at 430 MH_3. The position angle is a composite from work by Backer and Rankin (1980), Lyne, Smith, and Graham (1971), and unpublished data. The position angle at longitudes greater than 150° does not always increase as shown by the filled circles; sometimes it follows the dashed curve. This variation is probably due to a mixture of two othogonal polarization modes, whose relative strength varies over a timescale equal to that for computing the average (2083 pulses).

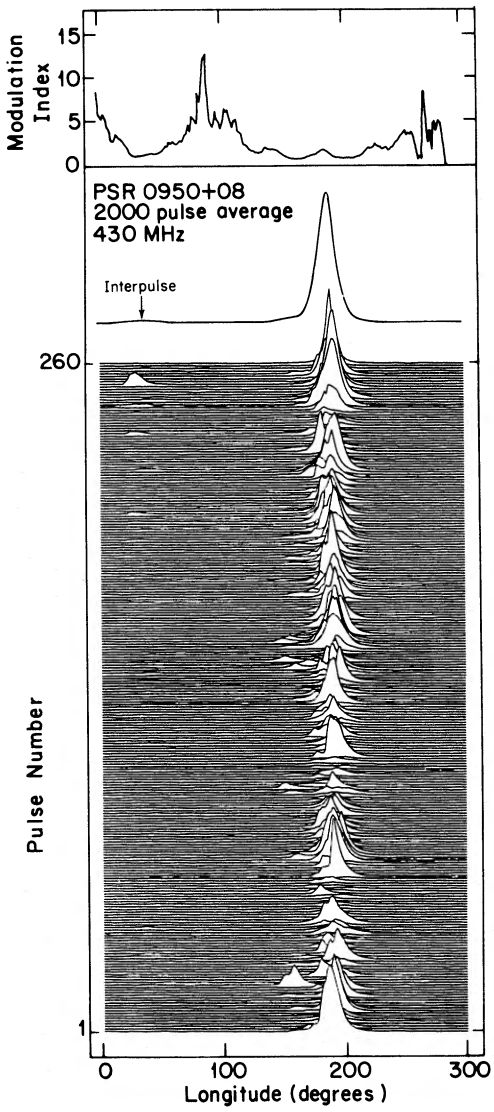

FIG. 5.—A sequence of 260 pulses that shows strong subpulses at the position of the interpulse. Also plotted is the modulation index [eq. (1)].

IV. MAIN PULSE AND INTERPULSE FLUCTUATIONS

a) Subpulse Fluctuations

It is well known that average intensity profiles measure both the average *strength* and the *frequency of occurrence* of pulse features (subpulse and micropulses). Figure 5 is a sequence of 260 pulses in which it is clear that the most intense single pulses occur near the peak of the average profile but that intense subpulses occasionally occur near the leading edge of the main pulse and even at the longitude of the interpulse. Also plotted in the figure is the modulation index

$$m = (\sigma_{on}^2 - \sigma_{off}^2)^{1/2}/(\langle I_{on}\rangle - \langle I_{off}\rangle)\,, \qquad (1)$$

where σ_{on}, σ_{off} are the on-pulse and off-pulse standard deviations of the intensity, $\langle I_{on}\rangle$ is the average on-pulse

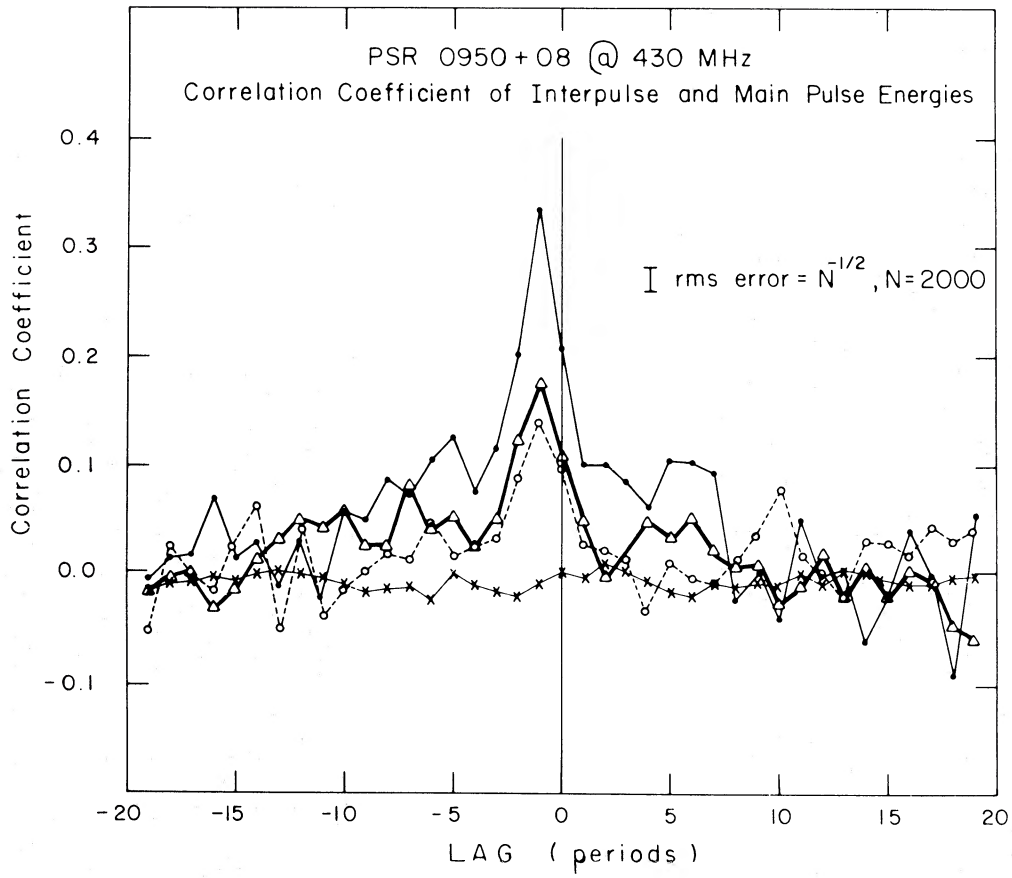

FIG. 6.—The correlation coefficient of interpulse and main pulse energies calculated for 3 independent sets of 200 pulses, as denoted by the open circles, filled circles, and triangles. There is no significant correlation between the main pulse and bridge energies (*crosses*).

intensity, and $\langle I_{\rm off} \rangle$ is the minimum value of the average profile. The modulation index is large when subpulses show either a large variation of intensity or if subpulses occur infrequently.

A correlation between main pulses and interpulses was revealed by calculating the mean interpulse intensity and mean main pulse intensity for each pulse and forming the cross-correlation function (CCF) of the two time series. The results shown in Figure 6 for several blocks of 2000 pulses indicate that the correlation coefficient is maximized at a lag of -1 period. That is, *a strong main pulse is followed* $\sim$ *140 milliseconds later by a strong interpulse.* One must ask whether the correlation coefficient is dominated by a few strong interpulses. The result is repeatable between several independent blocks of 2000 pulses, suggesting that the result is systematic. Moreover, the histograms of the mean intensities in Figure 7 indicate that interpulses occur with a continuum of intensities and that the number of average size interpulses ($\sim 2\%$ of the average main pulse intensity) is larger than the number of strong interpulses ($\sim 50\%$ of the average main pulse) by a factor greater than 10^3. Therefore, *the average sized interpulses dominate the calculated correlation functions.*

The established correlation between main pulses and interpulses may reflect drifting subpulses behavior whereby subpulses first seen in the main pulse appear in the interpulse ~ 140 ms later. An empirical test of this hypothesis is difficult. One would expect subpulses to appear in the bridge between main pulse and interpulse. A cross-correlation analysis performed on main pulse and bridge intensities showed no significant correlation at any lag. This may not argue against the drifiting subpulse hypothesis, however, because subpulses seen in the main pulse will appear in the bridge after a time less than one period, i.e., when the pulsar beam (in the polar cap model) is not directed towards the Earth.

b) Micropulse Structure

Micropulses with durations from ~ 10 μs to ~ 200 μs were identified in the main pulse (Hankins 1971, 1972) both by inspection of single pulse intensities and by detecting a systematic feature in the intensity autocorrelation function. Recently, Hankins and Boriakoff (1980) have discovered micropulses in the interpulse with a characteristic autocorrelation width ~ 90 μs at 430 MHz compared with a 130 μs value for the main pulse.

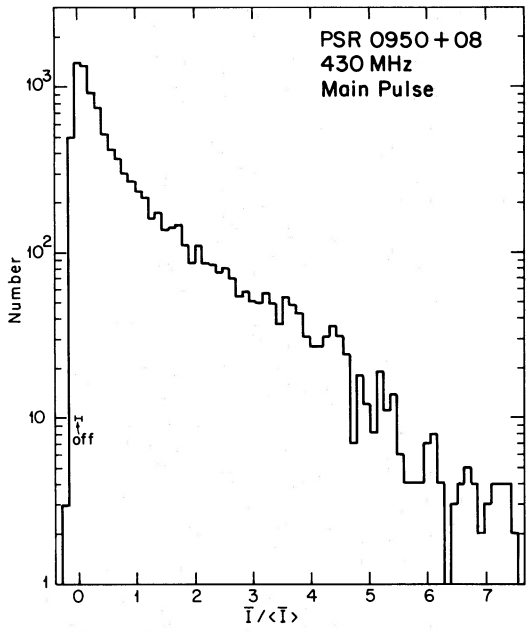

FIG. 7a

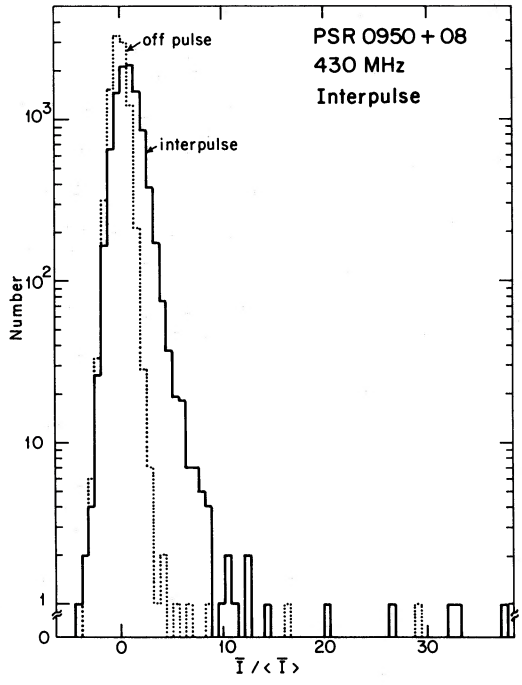

FIG. 7b

FIG. 7.—Histograms of mean pulse intensities for the main pulse and interpulse components and for a nominal offpulse portion of pulse longitude, calculated from 9600 pulses. The histograms are of the quantity $\bar{I}$, the average intensity in the relevant component in a single pulse. The horizontal scale is normalized to the mean average intensity over 9600 pulses, $\langle \bar{I} \rangle$.

V. CONSISTENCY WITH SINGLE POLE AND DOUBLE POLE INTERPRETATIONS

Interpulses were initially interpreted as emission from the "opposite" magnetic pole for two reasons: (1) they occur at a large ($\gtrsim 150°$) longitude separation from the main pulse, and (2) emission from single poles appeared to be confined to much smaller ($\lesssim 25°$) longitude regions. Manchester and Lyne (1977) pointed out that emission from the Crab pulsar, whose interpulse and main pulse are of approximately equal amplitude (in the radio), and the Vela pulsar, whose optical and γ-ray interpulse and main pulse do not appear in the radio, can more easily be understood as arising from a single pole. The main arguments in favor of a single pole model for Crab and Vela are: (1) a bridge of emission connects the main and interpulse components; (2) the main pulse–interpulse component separation is frequency dependent for the Vela pulsar; and (3) a histogram of component separations for many pulsars no longer appears to be bimodal, suggesting that both large and small component separations can be produced by the same mechanism.

The results on PSR 0950+08 contradict our expectations from both a single-pole and the double-pole models. Table 2 lists the supporting evidence for each kind of model along with the problems that each faces.

TABLE 2

EVIDENCE FOR AND AGAINST INTERPULSE MODELS

Model	Supporting Evidence	Problems
Single pole	$\Delta\theta^a = 150°$ (not 180°) bridge of emission; monotonic rotation of polarization position angle through $\lesssim 180°$.	Frequency independence of $\Delta\theta$; bifurcation of main pulse; amplitude difference of main and interpulse; (why no pulsars with four components?).
Double pole	Frequency independence of $\Delta\theta$; frequency dependence of *all* other separations; microstructure in both interpulse and main pulse; 2 poles predicted by polar cap models.	$\Delta\theta^a = 150°$ (not 180°); monotonic rotation of polarization position angle through $\lesssim 180°$; communication between poles necessary.

[a] $\Delta\theta$ = main pulse–interpulse separation in degrees longitude.

a) *Single-Pole Models*

The bridge of emission between main pulse and interpulse and a component separation significantly different from 180° are two points in favor of a single-pole model for PSR 0950+08. However, the frequency independence of the main pulse–interpulse separation, in contrast to the frequency dependent bifurcation of the main pulse, are difficult to understand in this model. Furthermore, the interpulse of PSR 0950+08 is much smaller than the main pulse, in contrast to the nearly equal main pulses and interpulses for the Crab and Vela pulsars.

In the single-pole model one must explain the wide cone angle (150°) as well as its frequency independence. We imagine three versions of the model for producing wide cone angles.

i) *High Altitude Interpulse Emission*

Suppose (Fig. 8*a*) that the bifurcated main pulse is produced close to the star near the magnetic pole, the bifurcation arising from a hollow cone beam that receives general support from pulsar observations (Backer 1976). The interpulse is then produced at a large radius where magnetic field lines have swept back such that the field line tangent makes a 150° angle with the magnetic pole.

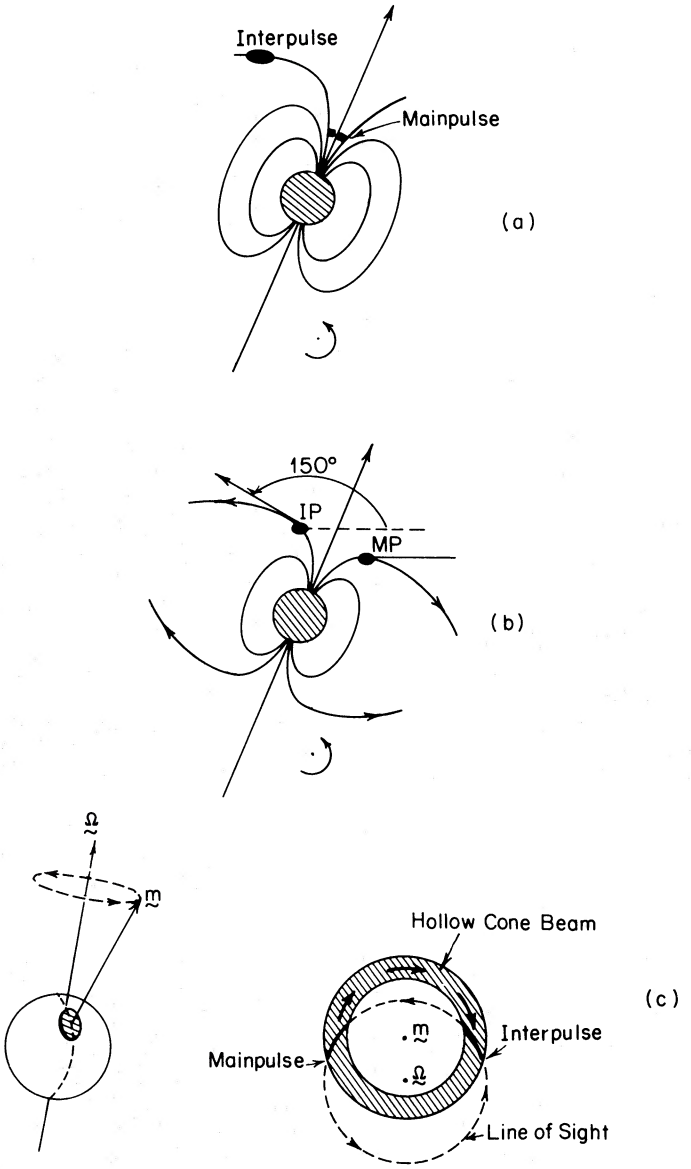

FIG. 8.—Single-pole models for the emission of PSR 0950+08. (*a*) Mainpulse emission arises in a hollow-cone beam, and the interpulse originates at a higher altitude. The rotation axis is perpendicular to the plane of the figure. (*b*) The large separation (150°) of the main pulse and interpulse is due to high altitude emission from both components. (*c*) Hollow cone beam centered on the magnetic pole (***m***) for a nearly aligned rotator. The arrows in the shaded path designate the drift path of particle sources (sparks), and the dashed line is the path of the line of sight around the rotation axis (**Ω**).

Such an emission region may be related to outer vacuum gaps suggested by Cheng, Ruderman, and Sutherland (1976). Emission processes in the main pulse and interpulse regions might be expected to be different. This model must then explain why micropulses of similar behavior appear in both the main pulse and interpulse (Hankins and Boriakoff 1980).

ii) *High Altitude Emission for Interpulse and Mainpulse*

An alternative (Fig. 8*b*; also discussed by Arons 1979) would explain the interpulse and main pulse as the result of the line of sight cutting through a hollow cone beam which would have a large opening angle due to the large radius ($\theta \propto r^{1/2}$). The main pulse bifurcation and its frequency dependence would then have to be confronted. At large radii, one may expect distortion of the dipolar field due to displacement and charge currents. PSR 0950+08 has a period derivative, $\dot{P} \approx 0.23 \times 10^{-15}$ s^{-1}, that is smaller than most pulsars with periods ~ 0.25 s. The implied surface magnetic field strength is 2.4×10^{11} gauss, if a dipolar field is assumed and for a moment of inertia of 10^{45} g cm^2. Consequently, the cone angle may be sufficiently large at radii smaller than the aberration limit (Cordes 1978) to produce the observed main pulse–interpulse separation. Arons (private communication) suggests that if one discards the assumption of a radius-to-frequency mapping, and hence also the aberration limits, then it is quite simple to get a wide hollow cone beam. However, the main pulse bifurcation must then be attributed to chance effects, which seems unsatisfactory because the main pulse shares a behavior that is common to many pulsars.

iii) *Emission from a Nearly Aligned Rotator*

Another model that produces large *observed* component separation is the case of the magnetic axis being nearly aligned with the rotation axis (Fig. 8*c*). The radio beam for such objects sweeps out a solid angle much smaller than do orthogonal rotators, but if the beam is directed at all toward the Earth, it is likely that it will be for a large fraction of the rotation period. Assuming that a hollow cone beam is centered on the magnetic pole, the interpulse and main pulse result when the line of sight enters and leaves the beam. The main pulse bifurcation clearly implies that the beam itself has frequency dependent structure, but it is difficult to understand why it is not also manifested in the interpulse.

The main pulse–interpulse correlation with a one period lag (§ VI) can be understood in this case as the drift of charge injection regions around the polar cap, as do the sparks in the Ruderman and Sutherland (1975) and Cheng and Ruderman (1980) models. Sparks in these models are localized regions of copious pair production that drift around the magnetic axis owing to an $\boldsymbol{E} \times \boldsymbol{B}$ drift. The absence of any observed bridge-mainpulse correlation can be understood if (as in Fig. 8*c*) sparks (denoted by arrows) that appear in the main pulse drift so as to intersect the line of sight next at the location of the interpulse region. The circulation period for a spark (Ruderman and Sutherland 1975) is

$$P_3 \approx 6B_{12}P^{-1}\,, \tag{2}$$

where B_{12} is the surface field in units of 10^{12} gauss, and P is the period. For PSR 0950+08 the sparks must drift approximately one-half the circumference of the polar cap in a time

$$\Delta t \approx P_3/2 \approx 12B_{12}s\,, \tag{3}$$

and we must have $\Delta t \approx P \approx 0.25$ or $B_{12} \approx 0.21$. This value is inconsistent with the $10^{11.4}$ gauss field determined from the equation appropriate for magnetic-dipole radiation,

$$B = (P\dot{P}Ic^3/4\pi^2R^6)^{1/2}\,,$$

where I is the moment of inertia (10^{45} g cm^2), and R is the stellar radius (10 km). It is not clear whether the discrepancy in magnetic fields should be resolved with simple changes in I and R or by modifying equations (2) and (4) for realistic magnetic field structures, etc.

b) Double-Pole Models

The frequency independence of $\Delta\theta$, the main pulse–interpulse separation, is the chief point in favor of a double-pole model. Most components that appear to be associated with a single pole are observed to have frequency dependent separations over *some* frequency range; the PSR 0950+08 main pulse–interpulse is a notable exception. To make this model work, one must explain the fact that $\Delta\theta = 150°$ by proposing that the two magnetic poles are not collinear or that the particle flow or the radiation beams are otherwise distorted. The observed main pulse interpulse correlation moreover implies a *unidirectional* communication between poles. That is, suppose a disturbance at the main pulse polar cap excites the interpulse polar cap via particles traveling along just-closed field lines that bound the open field line region (e.g., field line *a* in Fig. 9*a*). The diameter of such a path is approximately the light cylinder radius (at most), $r_{LC} = cP/2\pi$, so the propagation time is $\Delta t \lesssim \pi r_{LC}/c = P/2$, whereas strong interpulses occur $\sim 0.6P > P/2$ after strong main pulses. What ever the excitation mechanism, it must result in emission nearly the same as main pulse emission because micropulses appear from both regions with similar parameters. One difference, however, is that the interpulse emission is 100% linearly polarized at 430 MHz, whereas main pulse emission is only $\sim 20\%$ polarized, on average (Backer and Rankin 1981). Flow in the opposite direction would cause strong main pulses to follow strong interpulses, but that is not observed. Consequently, there is an observed asymmetry between the two polar caps.

Magnetosphere models indeed predict an asymmetry between the poles of orthogonal rotators (Sturrock 1971; Ruderman 1976; Arons and Scharlemann 1979). Figure 9 shows how the rotational equator divides the polar cap into zones of electron emission (+; those with $\boldsymbol{\Omega} \cdot \boldsymbol{B} > 0$) and ion emission (−). Some models associate radio emission with ion emission zones (Ruderman and Sutherland 1975), while other models (Arons 1981) attribute radio emission to electron zones. If PSR 0950+08 is an

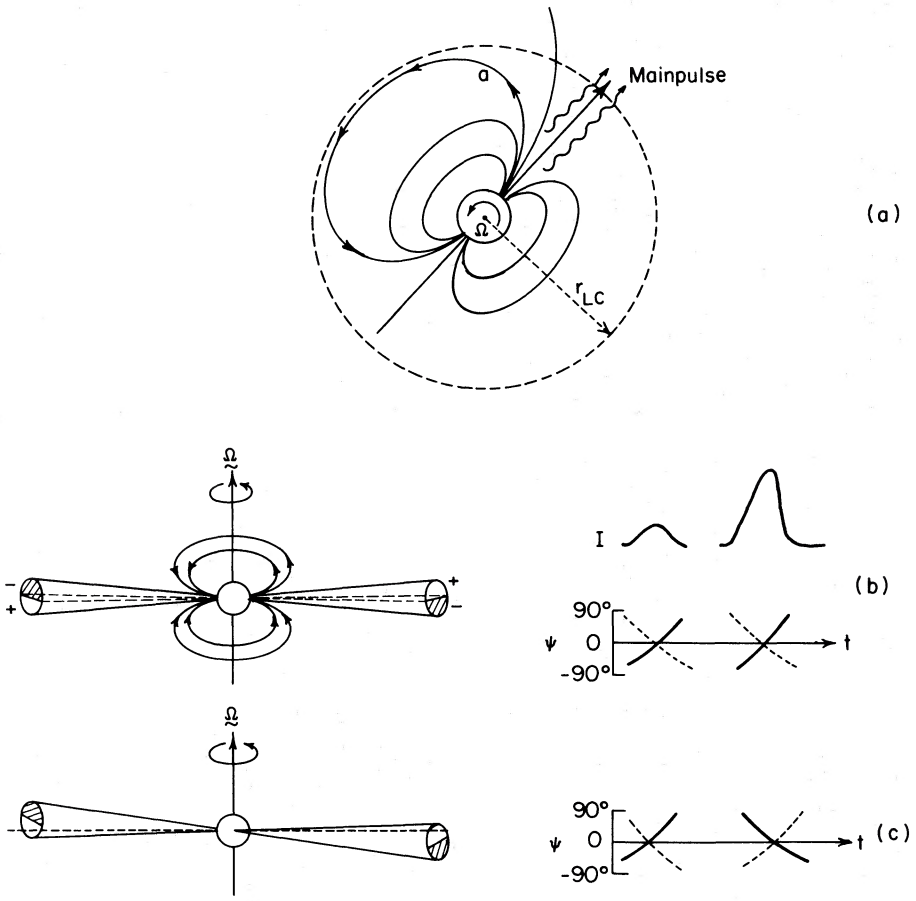

FIG. 9.—Double-pole models. (*a*) Main pulse emission at one pole with communication between poles along field *a*. (*b*) Orthogonal rotator ($\boldsymbol{\Omega} \cdot \boldsymbol{m} = 0$). The open field line regions have hemispheric structure such that field lines with $\boldsymbol{\Omega} \cdot \boldsymbol{B} > 0$ are sources of electrons (+), whereas those with $\boldsymbol{\Omega} \cdot \boldsymbol{B} < 0$ (−) are sources of ions. The polarization position angle is shown for the interpulse and main pulse. *Solid lines* (*dashed lines*): observer's line of sight sees upper (lower) halves of open-field line regions. (*c*) Nearly orthogonal rotator ($\boldsymbol{\Omega} \cdot \boldsymbol{m} \neq 0$). Line of sight now sees upper half of emission cone for one pole, lower half for other pole. The line of sight is assumed orthogonal to $\boldsymbol{\Omega}$. *Solid lines:* $\boldsymbol{\Omega} \cdot \boldsymbol{m} > 0$. *Dashed lines:* $\boldsymbol{\Omega} \cdot \boldsymbol{m} < 0$.

orthogonal rotator, then the main pulse and interpulse arise from two regions, one an electron zone, the other an ion zone. Explaining the main pulse–interpulse asymmetry in this way then leads us to the problem of how an interpulse region can produce essentially normal radio emission. Furthermore, polarization measurements (discussed below) are apparently in conflict with a two-pole model of this sort.

c) *Polarization Signatures*

The discussion thus far has concerned only the total intensity. Here we discuss the constraints that polarization measurements place on models. Of greatest importance is the position angle of the polarization ellipse, a quantity that appears to be determined by the ambient magnetic field of the star (Radhakrishnan and Cooke 1969). It can be shown that if the magnetic pole makes an angle α with the rotation axis and the angle between rotation axis and the line of sight is $\alpha + \sigma$, then the position angle is equal to the azimuthal angle of the line of sight with respect to the magnetic pole,

$$\psi(t) = \tan^{-1}[[[\sin(\alpha + \sigma)\sin(\Omega t)]/\{[\cos(\Omega t) - 1] \times \cos\alpha \sin(\alpha + \sigma) - \sin\sigma\}]] . \quad (5)$$

The pulse duration is the time over which the line of sight is at a magnetic polar angle less than the half-width of the radiation beam, θ_B,

$$\theta(t) = \cos^{-1}[\cos\sigma + (\cos\Omega t + 1)\sin\alpha \sin(\alpha + \sigma)] \leq \theta_B . \quad (6)$$

For single-pole models the observed 180° position angle rotation *and* large pulse width can both be produced if (1) the intrinsic beam width θ_B is large (i.e., $\theta_B \approx 150°$) and the "impact parameter" of the line of sight, σ, is small compared to θ_B; or (2) the intrinsic beam

width is small, but the magnetic pole is nearly aligned with the rotation axis: $\alpha \sim \sigma < \theta_B$. In the second case, the beam size may be, for example, that associated with the open-field-line region (Goldreich and Julian 1969) of a nearly aligned dipole:

$$\theta_B = \tfrac{3}{2}(r/r_{LC})^{1/2}, \quad (7)$$

which holds for $\theta_B \ll 1$, thus requiring the emission radius $r \ll r_{LC}$, as is consistent with retardation-aberration constraints (Cordes 1978). The observed pulse will extend through a large fraction of the period, $\Omega\Delta t = 150°$, if $\alpha \sim \theta_B$. The observed position angle variation requires σ to be a moderate fraction of θ_B, as shown in Figure 8*c*.

In double-pole models, the position angle variation is also described by equation (5), but variations may now extend through greater than 180° and/or may not be monotonic. In the orthogonal rotator of Figure 9*b*, the position angle varies *identically* in the main pulse and the interpulse; it is unmonotonic because, for equal sized radiation beams, position angles at the leading edges of the two components are the same. The nearly orthogonal rotator of Figure 9*c* has the position angle in the interpulse being the *time reverse* of that in the main pulse. The reason for this is that in one, the upper (relative to $\boldsymbol{\Omega}$) half polar cap, is seen; in the other the lower half polar cap is seen. Both of these position angle signatures are inconsistent with that observed. We take this as the strongest evidence *against* a double-pole model for PSR 0950+08.

d) The Crab Pulsar and PSR 0823+26

In contrast to PSR 0950+08, the position angle variation of the Crab pulsar (0531+21) in the optical (see Figs. 2 and 3 of Kristian *et al.* 1970) is in agreement with that expected from a double-pole orthogonal rotator in that, as in Figure 9*b*, the variation is almost the same in interpulse and main pulse. If a double-pole model holds for the Crab pulsar, then the appearance of the bridge of emission in X- and γ-ray emission negates the use of similar bridges in other objects as support for single-pole models.

In a recent study of PSR 0823+26 Backer and Rankin (1980) show that the polarization behavior is also consistent with a double-pole model of the kind of Figure 9*c*. While this pulsar has traditionally been attributed a single-lobed average profile, Backer and Rankin (1980) infer that a trailing weak component represents the second lobe of a double-lobe profile.

VI. DISCUSSION

The theoretical issues relevant to our observational results include: (1) the nature of large duty cycle emission in general and the cause of interpulses in particular; (2) whether frequency dependent pulse widths and separations are due to different frequencies originating at different radii; and (3) whether the tendency for pulse widths and separations to be frequency independent, or nearly so, above a certain frequency ($\sim$ 400 MHz for PSR 0950+08) signifies the existence of more than one emission mechanism.

a) Emission Filling the Entire Pulse Period

Small duty cycle emission is one among many of the supporting facts for polar cap models in which radiation is produced near the magnetic pole(s) and at a radius well within the velocity-of-light cylinder. In such models (e.g., Sturrock 1971; Ruderman and Sutherland 1975), particle flow is naturally confined to those magnetic field lines that connect outside the light cylinder. Consequently, large duty cycle emission such as that of PSR 0950+08 implies either (1) radiation occuring at radii comparable to the light cylinder radius or (2) radiation from a nearly aligned rotator so that a narrow beam points toward the Earth for a large fraction of the period.

In the first case, large radius emission would have the following consequences: (1) magnetic field lines will bend over large angles; (2) rotational aberration will smear emission over large angles; and (3) particles may have significant transverse momenta so that beaming will no longer be tangent to magnetic field lines. That is, the low level, large duty cycle emission may be similar to that expected from light cylinder models (e.g., Smith 1973). Such models generally ignore the particle flow that originates at the magnetic polar caps and do not convincingly (in our opinion) provide for the small duty cycle emission that is most prominent. However, light cylinder style emission indeed produce the observed low level emission. The main problem would be to provide a coherence-producing plasma instability that operates at large radii. (We note that although bridge emission is low level, its brightness temperature is still at least 10^{16} K).

The second case of a nearly aligned rotator would obviate the need for coming up with coherence mechanisms that operate over a large range of radii (e.g., small radii for main pulse emission, large radii for bridge emission). In our opinion, a nearly aligned rotator can explain the emission from PSR 0950+08 with virtually no difference in physics from arbitrary skewed rotators that can account for pulsars as a class of objects. There are no theoretical reasons against the magnetic and rotational axes being nearly aligned, nor does theory prevent such objects from being pulsars. In fact, Jones (1976*a*, *b*) has argued that the period–pulse-width distribution provides evidence for magnetic alignment occurring on timescales of 10^4–10^6 years.

The main snags with a nearly aligned rotator are the frequency independence of the main pulse–interpulse separation and the bifurcation of the main pulse contrasted with the single-lobed interpulse. However, of the models we have considered, we consider this model the easiest to modify to bring it into conformance with the data.

b) On the Radius-to-Frequency Mapping

Cordes (1978) has reviewed the evidence for emission at a given radius being confined to a small (relative to the observed spectrum) range of frequencies. The variation of pulse widths as $\nu^{-\alpha}$ with $0.1 \lesssim \alpha \lesssim 0.6$ below a cutoff frequency ν_c is one of the prime sources of support (Komesaroff 1970). Furthermore, the consistency of

dispersion measurements with the cold plasma dispersion law (Craft 1970) implies that the *midpoints* of average profiles are to be associated with an axis of symmetry of the radiation beam, which is likely to be the magnetic pole. The main pulse of PSR 0950+08 conforms to Craft's conclusions, and therefore a nearly aligned rotator, for which the axis of symmetry would be between the main pulse and interpulse, is difficult to understand. We again emphasize that the frequency independence of the main pulse–interpulse separation is quite unusual. This suggests that the main pulse and interpulse are not produced by a hollow cone beam such as those invoked to explain double-lobe average profiles in general (Backer 1976).

A histogram of average profile component separations (Manchester 1978; Arons 1979) shows a large peak at angles $\lesssim 30°$ and a small number extending out to 180°, the latter group including pulsars with interpulses. Arons (1979) and Arons and Scharlemann (1979) propose that the histogram can be explained with a single (hollow cone beam) model in which small (large) separations correspond to low (high) altitude emission. The observations of PSR 0950+08 discussed here present a notable counterexample to such a synthesis, however, because the main pulse–interpulse separation does not share the same behavior (especially the frequency dependence) with most of the smaller separations.

An obvious alternative is to associate the interpulse and main pulse *centroids* with regions that are fixed in angle and/or radius with respect to the star. The two magnetic poles in a double-pole model exemplify a fixed angle situation. On the other hand, a single-pole model with the main pulse centroid corresponding to the magnetic pole and the interpulse arising at a fixed radius outer vacuum gap (Cheng and Ruderman 1977) is another configuration that may explain the observations. As previously pointed out, the problem then is the explanation for micropulses appearing in both the interpulse and main pulse.

One possibility is that there are *two* axes of symmetry, one related to the dipolar component of the field, the other to a multipole component of the field. Arons (private communication) has pointed out that a radius-to-frequency mapping in a magnetic quadrupole will (if the emission frequency is proportional to the local plasma frequency) yield a pulse width that varies as $\nu^{-1/2}$, a variation that is consistent with that observed for the main pulse and interpulse (§ III).

c) *More than One Emission Mechanism?*

Single-pole models for interpulses have a tendency for necessitating more than one emission mechanisms. Manchester and Lyne (1977) suggested that the Crab pulsar's precursor and the Vela pulsar's lone radio component were akin to one mechanism, while the Crab main pulse and interpulse correspond to another. Our discussion above also points toward the existence of two mechanisms for PSR 0950+08 in a single-pole model, although the evidence is ambiguous since the main pulse and interpulse share the presence of microstructure.

We take the opportunity here to point out further evidence for multiple emission mechanisms. It has been found (Cordes 1975; Cordes, Weisberg, and Hankins 1980; Bartel *et al.* 1980) that four pulsars with drifting subpulses display a nondrifting emission component that dominates the pulses at high frequencies. There are reasons to believe that the weaker (sometimes negligible) variation with frequency of component separations above a cutoff frequency ν_c may be related in general to a high frequency emission component.

VII. CONCLUSIONS

We have found that (1) emission from PSR 0950+08 occurs over at least 83% of the rotation period; (2) individual interpulses are occasionally as strong as 60% of the average main pulse; (3) the average interpulse–main pulse ratio is 2%; (4) interpulse amplitudes are positively correlated with main pulses that precede them; (5) the interpulse–main pulse separation is frequency independent between 100 and 5000 MHz, whereas (6) the average interpulse and main pulse widths vary as $\nu^{-0.5\pm0.05}$ below 400 MHz. Another important result (Hankins and Boriakoff 1980) is that main pulses and interpulses both display micropulses with characteristic autocorrelation scales of 130 μs and 90 μs, respectively.

We have considered both single-pole and double-pole models and find that both require additional ad hoc additions to explain certain observations. It appears simplest, however, to modify single-pole models in which the magnetic axis is nearly aligned with the rotation axis.

We would like to thank J. Arons, D. Backer, J. Rankin, and J. Weisberg for helpful discussions. We thank D. A. Graham, D. Morris, J. Seiradakis, and W. Sieber for unpublished data from Effelsberg; V. Boriakoff, D. B. Campbell, D. C. Ferguson, and J. M. Rankin for some of the unpublished Arecibo data; and W. Collins for data reduction. J. Weisberg also helped in the data analysis leading to Figure 5. We thank the MPIAe for use of their 47 MHz feed at Arecibo Observatory. We thank I. Haeck, D. Stewart, and J. Kellogg for typing the manuscript. J. M. C. was supported in part by NSF grants MPS 75-03377 and ATS 75-23581 at the University of Massachusetts and by the National Astronomy and Ionosphere Center (NAIC). T. H. H. thanks the Alexander von Humboldt Stiftung for support during some of this work. Arecibo Observatory is operated by Cornell University under contract with the National Science Foundation.

REFERENCES

Arons, J. 1979, *Space Sci. Rev.*, **24**, 437.
———. 1981, *IAU Symposium No. 95, Pulsars*, ed. R. Wielebinski and W. Sieber (Dordrecht: Reidel), in press.
Arons, J., and Schalemann, E. T. 1979, *Ap. J.*, **231**, 854.
Backer, D. C. 1976, *Ap. J.*, **209**, 895.
Backer, D. C., Boriakoff, V., and Manchester, R. N. 1973, *Nature Phys. Sci.*, **243**, 77.
Backer, D. C., and Rankin, J. M. 1980, *Ap. J. Suppl.*, **42**, 143.

———. 1981, to be submitted.
Bartel, N. *et al.* 1980, *Astr. Ap.*, in press.
Cheng, A., and Ruderman, M. 1980, *Ap. J.*, **235**, 576.
Cheng, A., Ruderman, M. A., and Sutherland, P. G. 1976, *Ap. J.*, **203**, 209.
Cordes, J. M. 1975, *Ap. J.*, **195**, 193.
———. 1978, *Ap. J.*, **222**, 1006.
Cordes, J. M., and Hankins, T. H. 1977, *Ap. J.*, **218**, 484.
Cordes, J. M., and Rickett, B. J. 1981, to be submitted.
Cordes, J. M., Weisberg, J. M., and Hankins, T. H. 1981, *Ap. J.*, submitted.
Craft, H. D., Jr. 1970, Ph.D. thesis, Cornell University.
Downs, G. S. 1979, *Ap. J. Suppl.*, **40**, 365.
Goldreich, P., and Julian, W. H. 1969, *Ap. J.*, **157**, 869.
Hankins, T. H. 1971, *Ap. J.*, **169**, 487.
———. 1972, *Ap. J.* (*Letters*), **177**, L11.
Hankins, T. H., and Boriakoff, V. 1978, *Nature*, **276**, 45.
———. 1980, preprint.
Izvekova, V. A., Kuzmin, A. D., Malofeev, V. G., and Shitov, Ju. P. 1979, *Soviet Astron.*, **23**, 179.
Jones, P. B. 1976*a*, *Nature*, **262**, 120.
———. 1976*b*, *Ap. J.*, **209**, 602.
Komesaroff, M. M. 1970, *Nature*, **225**, 612.
Kristian, J., Visvanathan, N., Westphal, J. A., and Suellen, G. H. 1970, *Ap. J.*, **162**, 475.
Lyne, A. G., Smith, F. G., and Graham, D. A. 1971, *M.N.R.A.S.*, **153**, 337.
Manchester, R. N. 1971, *Ap. J. Suppl.*, **23**, 283.
———. 1978, *Proc. Ast. Soc. Australia*, **3**, 200.
Manchester, R. N., and Lyne, A. G. 1977, *M.N.R.A.S.*, **181**, 761.
Radhakrishnan, V., and Cooke, D. J. 1969, *Ap. Letters*, **3**, 225.
Rickett, B. J., Hankins, T. H., and Cordes, J. M. 1975, *Ap. J.*, **201**, 425.
Rickett, B. J., and Lyne, A. G. 1968, *Nature*, **218**, 934.
Ruderman, M. 1976, *Ap. J.*, **203**, 206.
Ruderman, M., and Sutherland, P. G. 1975, *Ap. J.*, **196**, 51.
Sieber, W., Reinecke, R., and Wielebinski, R. 1975, *Astr. Ap.*, **38**, 169.
Smith, F. G. 1973, *Nature*, **243**, 207.
Sturrock, P. A. 1971, *Ap. J.*, **164**, 529.
Taylor, J. H., Manchester, R. N., and Huguenin, G. R. 1975, *Ap. J.*, **195**, 513.

JAMES M. CORDES: Space Sciences Building, Cornell University, Ithaca, NY 14853

TIM H. HANKINS: Arecibo Observatory, P.O. Box 995, Arecibo, PR 00612